Microstructural aspects of high temperature deformation of monocrystalline nickel base superalloys: some open problems

H. Mughrabi*

Some open questions concerning the microstructural mechanisms which govern the high temperature strength of monocrystalline nickel base superalloys will be reviewed in the context of previous work. Emphasis will be laid on microstructural effects observed in microyielding, creep, isothermal and thermomechanical fatigue and on the role of the γ/γ' lattice misfit with respect to γ/γ' rafting. The conditions for cutting of the γ' rafts will be stated in a simplified two-dimensional dislocation model. Effects of the connectivity of the coarsened γ/γ'microstructure and of the orientation of γ/γ' rafts on the strength properties will be discussed, and potentially beneficial effects of a positive lattice misfit will be addressed. Attention will be drawn to counteracting alloying effects which modify both the lattice mismatch and the diffusion kinetics. The main conclusion is that the optimisation of superalloy properties can only be sought in improving the most important properties without deterioration of other desirable properties.

Keywords: Monocrystalline nickel-base superalloys, Lattice misfit, High temperature creep and fatigue, Rafting, Diffusion kinetics, Alloying effects

Dedicated to the memory of Professor Malcolm McLean

Introduction

Because of their outstanding high temperature strength, nickel base superalloys have been and still are the most important materials for use in turbine components.[1,2] In particular, the use of nickel base superalloys in monocrystalline form has become more and more common. The superior strength properties result from the combined effect of precipitation hardening by a high volume fraction of the ordered coherently embedded γ' particles and the strong solid solution hardening of the γ matrix phase. The microstructural stability of the two-phase γ/γ' structure under severe mechanical and thermal loading is another important key property. In the past, the high temperature creep and fatigue behaviours of monocrystalline nickel base superalloys have been investigated in considerable detail, and in many cases a good understanding has been achieved, as summarised in some reviews.[3–6] Among the many contributions to the study of nickel base superalloys, some of the work of Malcolm McLean to whom this article is dedicated deserves to be mentioned.[7–9] Nonetheless, in view of the different varieties of alloys considered and the complexity of the microstructural deformation processes under different conditions of stress and temperature, several open questions remain. Some of these questions have been studied on different monocrystalline nickel base superalloys in the author's research group in the last 15 years. In the present work, these studies will form the basis of an attempt to establish links between the insights obtained and to draw some more general conclusions that could motivate further studies.

The following microstructural aspects of the high temperature strength of monocrystalline nickel base superalloys will be addressed:

- dislocation processes during microyielding at different temperatures
- effect of γ/γ' lattice misfit δ on the high temperature creep strength
- mechanism and effects of directional coarsening, i.e. rafting of the γ/γ' microstructure: role of plastic strain; effects of connectivity of γ/γ' microstructures; effect on creep strength and effect on fatigue strength
- potentially beneficial effects of a positive γ/γ' lattice mismatch
- competition between alloying effects on the driving force for coarsening and on the diffusion kinetics
- is there an optimum design strategy to develop superior nickel base superalloys?

γ/γ' lattice misfit and coherency stresses

Monocrystalline nickel base superalloys usually solidify in an orientation that lies close to one of the <001> directions which is usually referred to as [001]. In the cast and heat treated condition, the γ' particles have a cuboidal shape with an edge length in the order of 0·5 μm and are embedded coherently in the γ matrix. Since the γ' particles occupy a large volume fraction of 60–70%, the γ matrix channels between the cuboidal γ'

Department of Materials Science and Engineering, General Material Properties, University of Erlangen Nürnberg, Martensstrasse 5, D 91058 Erlangen, Germany

*Corresponding author, email mughrabi@ww.uni-erlangen.de

Published by Maney on behalf of the Institute
Received 26 June 2008; accepted 17 July 2008
DOI 10.1179/174328408X361436

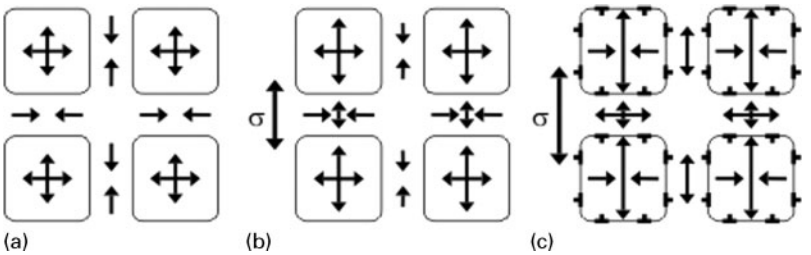

a initial coherency stresses; *b* superposition of coherency stresses with small external elastic tensile stress σ; *c* as *b*, for larger external stress σ, after small plastic deformation

1 Schematic illustration of stresses acting in superalloy with cuboidal γ' particles embedded in γ matrix channels: sizes of arrows indicate qualitatively magnitude of locally acting stresses (after Reichstein *et al.*[18,19])

particles are very narrow (~0·1 μm). Hence deformation of the channels by dislocation glide requires a high Orowan type bowing stress. In addition, the important role of the coherency stresses must be considered. The coherency stresses are directly related to the γ/γ' lattice misfit parameter δ which is defined as follows

$$\delta = \frac{a_{\gamma'} - a_{\gamma}}{2(a_{\gamma'} + a_{\gamma})} \quad (1)$$

where a_{γ} and $a_{\gamma'}$ are the lattice constants of the γ and γ' phases, respectively. The γ/γ' lattice misfit parameter δ has frequently been considered as one of the most important microstructural parameters that govern the mechanical properties of superalloys (compare Refs. 3–6 and 10–17). Typically, δ is negative and in the order of -10^{-3} in many commercial superalloys and increases in magnitude with increasing temperature. The coherency stresses induce triaxial tensile stresses in the three <001> directions in the γ' particles and, in good approximation, biaxial compressive stresses in the γ channels in the <010> directions lying parallel to the bordering {001} planes, as indicated in Fig. 1*a* from Refs. 18 and 19. In the absence of an external stress, the stress states in the three types of (crystallographically equivalent) γ matrix channels are similar. However, once an external stress is applied, for example a small elastic tensile stress in the vertical [001] direction, then the superposition of the tensile external stress and the compressive coherency stresses will induce a different stress state in the horizontal channel than in the two vertical channels (compare Fig. 1*b*). If the applied stress is increased, plastic deformation would commence in the horizontal channels (Fig. 1*c*) as a result of the superposition of the biaxial compressive coherency stresses and the vertical tensile stress, and interfacial dislocations would accumulate at the horizontal γ/γ' interfaces.[3–6,10–15] On the other hand, yielding of the vertical channels with accumulation of interfacial dislocations at the vertical γ/γ' interfaces would be delayed because the applied tensile stress would be diminished by the vertical compressive coherency stress. These modifications of the stress state by the coherency stresses affect the glide modes in the microyielding stage, in particular at rather 'low' temperatures, as shown in section on 'Microyielding at different temperatures'. Moreover, they govern the mode of coarsening and the overall deformation behaviour at elevated temperatures, as will be detailed in section on 'Directional coarsening (rafting) at high temperatures'. This illustrates the important role played by coherency stresses and indicates why the importance of the γ/γ' lattice misfit has often been emphasised. At the same time, the discussion about the role of the lattice misfit has remained controversial till today.

Microyielding at different temperatures

The dislocation glide processes in the early stages of unidirectional deformation of monocrystalline nickel base superalloys have been studied by a number of different authors.[11,20–22] In these studies, a sequence of glide processes in the narrow γ matrix channels and sometimes cutting of the γ' particles could be identified. Subtle effects of the temperature dependence and its effects on the highly resolved stress–strain curves have not previously been investigated in sufficient detail. In a more detailed so far unpublished study, Reichstein *et al.*[18,19] investigated the microyielding behaviour of single crystals of the superalloy CMSX-6 which had been deformed in tension at a total strain rate $\dot{\varepsilon}_t = 6{\cdot}67 \times 10^{-5}\,s^{-1}$ up to total strains ε_t of 3% at temperatures of 900, 1000 and 1100°C respectively. Figure 2 shows the stress–strain curves in the forms stress σ versus total strain ε_t (Fig. 2*a*) and stress σ versus plastic strain ε_{pl} (Fig. 2*b*) respectively. The plastic strain was obtained by subtracting from the total strain the elastic strains which were calculated, using the temperature dependent Young's moduli. Several features are noteworthy. As expected, the stress levels decrease strongly with increasing temperature. At the two higher temperatures of 1000 and 1100°C, the stress–strain curves are rather smooth, whereas at the lowest temperature (900°C) the stress–strain curve exhibits distinct stages which are much more clearly visible in the σ versus ε_{pl} plot than in the plot of σ versus ε_t. It should be noted that in the σ versus ε_{pl} plot (in which the elastic line is vertical), the plastic strain extends only up to $\sim 6 \times 10^{-3}$. Within this small range of plastic strain, four distinct deformation stages (numbered in Fig. 2*b*) can be recognised easily. In passing, it is noted that in the limit of very low stresses the stress–strain curve at 900°C deviates into the range of negative strains. The reason for this unusual behaviour is not clear. However, it appears probable that this is not a real effect but that the elastic strain has been overestimated in the procedure of converting the total strains to plastic strains. The four deformation stages which appeared at the rather low temperature of 900°C are interpreted as follows:

Stage 1 dislocation glide occurs in the horizontal γ channels, accompanied by strain hardening, interfacial dislocations accumulate at the γ/γ' interfaces. This leads to the

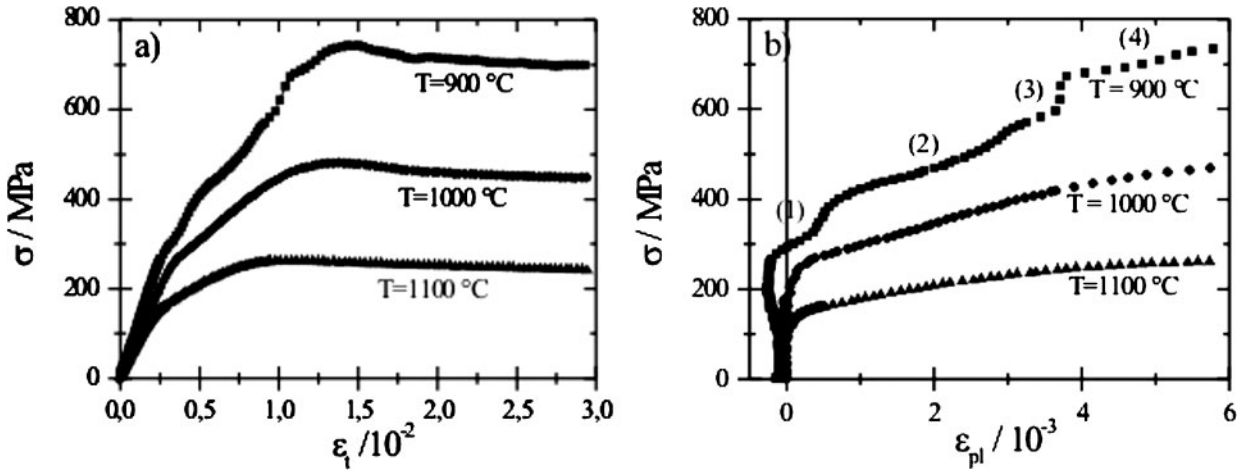

a plot of σ versus ε_t; *b* plot of σ versus ε_{pl}

2 Microyielding stress–strain curves of CMCX-6 monocrystals deformed in tension at total strain rate $\dot{\varepsilon}_t = 6{\cdot}67 \times 10^{-5}\ s^{-1}$ at temperatures of 900, 1000 and 1100°C up to total strains $\varepsilon_t = 0{\cdot}03$ (courtesy Reichstein *et al.*)[18,19]

building up of deformation induced transverse internal back (tensile) stresses in the γ channels and transverse internal 'forward' (i.e. compressive) stresses in the γ' particles

Stage 2 dislocation glide now occurs also in the vertical γ channels. Continued building-up of interfacial dislocations and internal stresses which are 'forward' in the γ' particles is compressive in the transverse direction and tensile in the direction of the applied stress

Stage 3 after the internal forward stresses in the γ' particles have become sufficiently large, some dislocations can cut the γ' particles, beginning at the horizontal γ/γ' interfaces

Stage 4 as deformation continues, γ' particles are now also cut by dislocations from the vertical γ/γ' interfaces.

In an independent study, Fedelich *et al.*[23] have modelled the microyielding stress–strain curves, based on similar considerations. At higher temperatures dislocations can circumvent the γ' particles and escape by climb, the discrete nature of the deformation stages is partially lost, and the stress–strain curves become smoother (compare Fig. 2*a*). Microstructural evidence of the processes described has been obtained by transmission electron microscopy (TEM). At a deformation temperature of 900°C (Fig. 3*a*), the accumulation of dislocations at the γ/γ' interfaces and the cutting of γ' particles, evidenced by the stacking fault contrast (seen in the top right corner), can be recognised. At the higher temperature of 1000°C (Fig. 3*b*), the most important change seen in addition to the interfacial dislocations is the rounding-off of the corners of the γ' particles. This indicates that at this temperature diffusional mass transport is occurring. Finally, at the highest temperature of 1100°C, the rounded γ' particles begin coalescing to form elongated platelike particles lying roughly perpendicular to the vertical stress axis. This process can be considered as a precursor of directional coarsening or rafting (compare Refs. 3–16 and 20–29), which is known to occur in the form of γ/γ' plates lying roughly perpendicular to the stress axis in the case of superalloys with negative γ/γ' lattice misfit δ. At the temperature of 1100°C, the observations show no evidence of cutting of γ' particles but indicate that the particles are circumvented by climb. According to a simple estimate of the climb velocity,[19] this appears reasonable. One minor point should be noted. In their study on a model monocrystalline superalloy and the superalloy NASAIR 100, Gabb

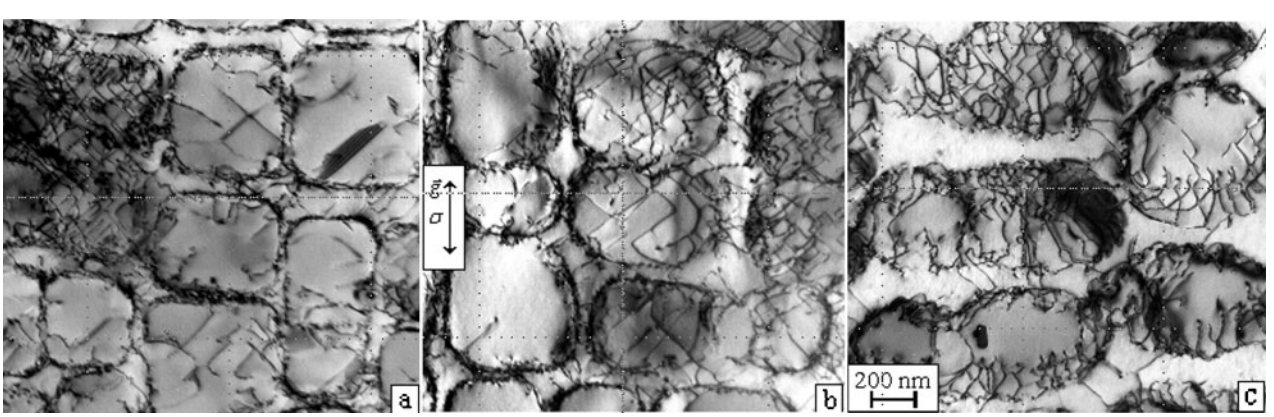

3 Images (TEM) showing dislocation distributions in (010) sections of CMSX-6 single crystals after tensile deformations at temperatures of *a* 900°C, *b* 1000°C and *c* 1100°C to total strains $\varepsilon_t = 0{\cdot}03$: cutting of γ' particles and rounding-off of corners at 1000°C and coarsening and coalescence at 1100°C should be noted. The stress axis and the direction of the diffraction vector g lie in the verticle direction, as indicated (courtesy Reichstein *et al.*[18,19])

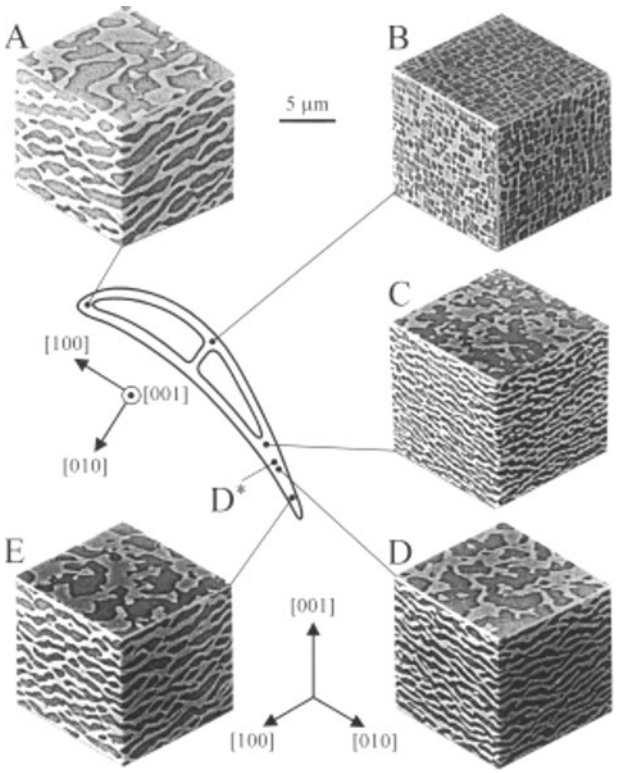

4 Three-dimensional montages of SEM study of local γ/γ' microstructures at different locations of turbine blade that had been subjected to 'accelerated mission test' under service conditions for several hundreds of hours: shape of blade has been modified for proprietary reasons (from von Grossmann *et al.*)[32]

et al. found that 'dislocations were not required at the γ' interfaces which coalesced to produce rafts'.[10] While this finding differs from that of Reichstein *et al.*, it probably indicates that such details depend on the particular alloy investigated.

To summarise, the experimental evidence shows that microyielding at not too high temperatures occurs in distinct stages through a sequence of glide processes. These stages of microyielding are reflected in subtle details of the stress–strain curve, and can be interpreted in terms of specific dislocation glide processes which can be identified by TEM.

Directional coarsening (rafting) at high temperatures

Rafting in high temperature creep

The phenomenon of directional coarsening, i.e. rafting, of the γ/γ' microstructure during high temperature deformation has fascinated many researchers and motivated extensive studies (compare Refs. 7–13, 16 and 20–29 and the reviews of Refs. 3–6, 14 and 15). Nonetheless, some aspects concerning the mechanism of rafting and the effect of rafting on the high temperature strength properties are still under discussion. For example, there are exceptions to the general assumption that in alloys with a negative γ/γ' lattice misfit, rafts form perpendicular to the stress axis when the stress is tensile and parallel to the stress axis for compressive stresses. More strictly speaking, it is important to consider in addition that rafting inevitably requires a small plastic

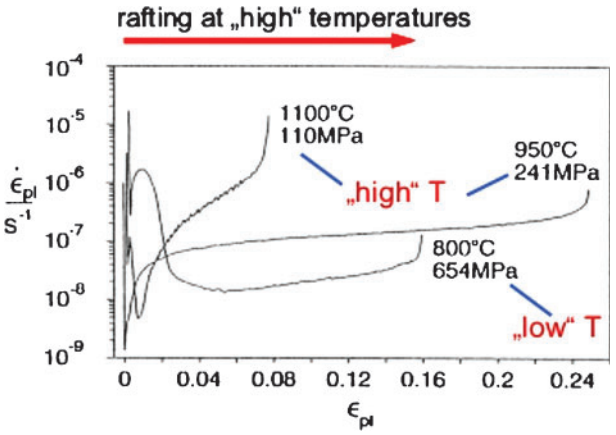

5 Examples of creep deformation curves of single crystals of superalloy CMSX-4 at temperatures of 800, 950 and 1100°C, plotted in form $\dot{\varepsilon}_t$ versus ε_{pl} (from Schneider *et al.*)[33,34]

strain and that under more complex loading conditions, and there are more signs of the plastic strain than the stress that governs whether the rafts form parallel or perpendicular to the stress axis. This will be discussed in the next section. While such details may be of academic nature, the practical implications of rafting follow simply from the facts that rafting is known to occur in turbine blades under service conditions (as first shown by Draper *et al.*,[30] see also Refs. 31 and 32), and that rafting can deteriorate the creep resistance. In turbine blades, rafting occurs during the very small high temperature creep deformation that the blade undergoes in response to the centrifugal force. Figure 4, from the work of von Grossmann *et al.*,[32] shows three-dimensional (3D) montages of micrographs of the γ/γ' microstructures observed by scanning electron microscopy (SEM) in a turbine blade made of the superalloy CMSX-6 that had been subjected to a so called accelerated mission test for several hundreds of hours in a test turbine. The section investigated lay at ~30% of the total height of the airfoil. Severe rafting at the leading and the trailing edges is observed, with strong coarsening at the leading edge, while the initial cuboidal γ' microstructure is still largely retained in the middle part near the cooling channels.

In a creep test, the formation of rafts is favoured by rather high temperatures (~1000°C) and low stresses (i.e. also low strain rates). Therefrom, it can be concluded that rafting is a time dependent high temperature diffusion controlled process. In this context, it is instructive to compare the shapes of creep curves observed under different conditions of stress and strain. In Fig. 5, three creep curves from the work of Schneider *et al.*[33,34] on specimens of the second generation superalloy CMSX-4 at 800, 950 and 1100°C are compared. The creep curves are presented in differentiated forms, i.e. in plots of plastic strain rate $\dot{\varepsilon}_{pl}$ versus ε_{pl}, since subtle details are much more easily recognisable in this kind of plot than in the also very common ε versus t plots (t: time). It is immediately obvious that all three creep curves have a rather complex shape, in particular during the first few percent of strain. As shown in more detail elsewhere,[28,33] γ/γ' rafting is only observed at the two 'high' temperatures of 950 and 1100°C (and the rather 'low' stresses of 241 and 140 MPa

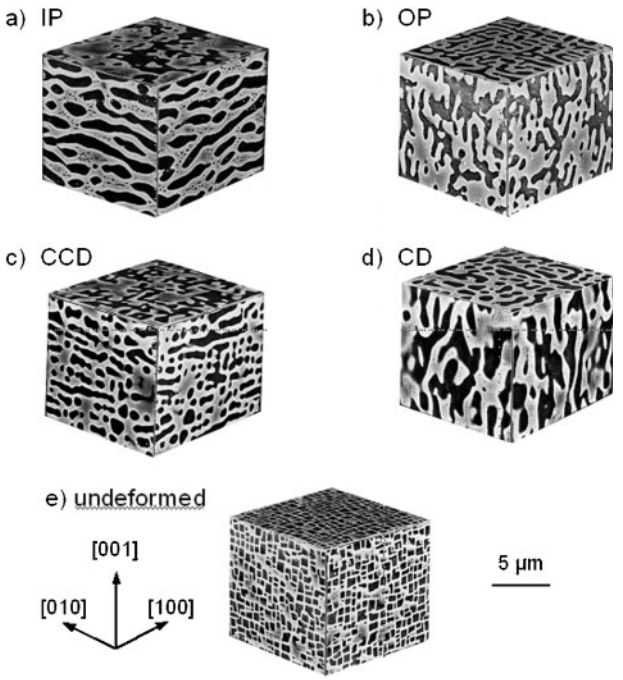

a in-phase TMF; *b* out-of-phase TMF; *c* counterclockwise diamond TMF; *d* clockwise diamond TMF; *e* initial γ/γ' microstructure

6 Three-dimensional montages of SEM study of γ/γ' microstructures of single crystals of superalloy CMSX-6 after TMF under different loading conditions (after Kraft *et al.*)[35]

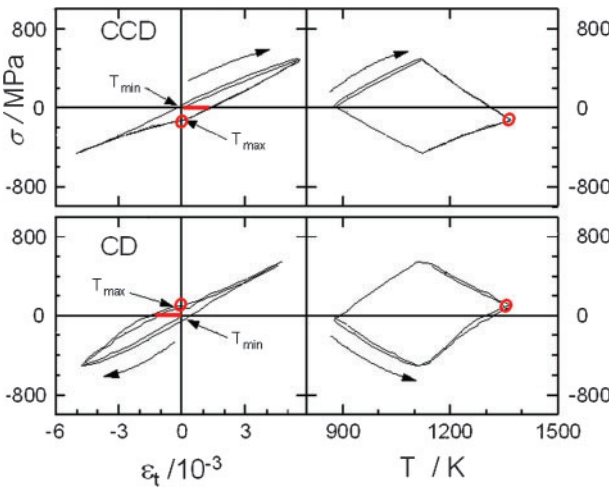

7 Plots of stress σ versus ε_t and σ versus temperature T for CMSX-6 single crystals subjected to TMF loading with CCD and CD cycles (after Kraft *et al.*)[35]

respectively), whereas at the 'low' temperature of 800°C (and the rather 'high' stress of 842 MPa) the γ' particles are cut by the dislocations and retain their cuboidal shape.

For the subsequent discussion whether γ/γ' rafting is beneficial or damaging for the creep strength, it is interesting to note the following with respect to the creep behaviour of CMSX-4 (compare Fig. 5).[28,33] At 950°C, rafting begins after <1% of plastic strain when the minimum creep rate has been attained. As rafting proceeds, the creep rate increases sharply, indicating that the material is actually softening. In the later stages of deformation, the creep rate continues to increase more moderately but persistently as the rafts coarsen. In contrast, at 1100°C, the beginning of rafting is accompanied by softening, as indicated by an increase in the creep rate after it has passed through the first minimum. Then, however, rafting continues as the creep rate decreases a second time, i.e. as hardening occurs. When the creep rate has reached its second and absolute minimum, rafting is completed. The second increase in the creep rate is related to the softening that occurs in connection with the subsequent coarsening of the γ/γ' raft microstructure.

Rafting in thermomechanical fatigue

The severe changes in temperature and stress that occur at the (leading) edges of turbine blades during start-up and shut-off procedures of the engine are simulated in the laboratory in so called thermomechanical fatigue (TMF) tests. In such TMF tests, the specimen is subjected to cycles of simultaneous changes of stress and temperature for different phase relations. The two extreme cases are so called in-phase TMF, during which the tensile (compressive) stress increases as the temperature increases (decreases) and out-of-phase TMF tests with the stress increasing (decreasing) with decreasing (increasing) temperature. Rafting is of course assumed to occur when the temperature is maximum. In TMF tests on the superalloy CMSX-6,[35] conducted with upper and lower temperatures of 1100 and 600°C respectively, rafting was observed for both in-phase and out-of-phase cycles in accord with expectation. In other words, the rafts formed perpendicular or parallel to the stress axis at the high temperature when the stress was tensile or compressive respectively. A particularly interesting and instructive observation was made in the case of so called diamond cycles, with phase angles of $\pi/2$ (counterclockwise diamond: CCD) or $3\pi/2$ (clockwise diamond: CD) between strain and temperature. The terms CD and CCD refer to the sense of the cycle in a plot of temperature T versus total strain ε_t. In passing, it is noted that the CCD cycle is considered to be particularly suited to simulate the conditions at the leading edge of a blade.[36] In the TMF tests on the alloy CMSX-6, rafting was found to occur in both CD and CCD TMF tests (*see* Fig. 6). However, for this more complex form of loading and as becomes evident more clearly, when considering the cycle shapes either as stress σ versus total strain ε_t or as stress σ versus temperature T (as shown in Fig. 7), the type of rafting observed is contrary to expectation, if one considers only the sign of the stress at the highest temperature. As shown on the left and right sides of the figure, the stress is negative at the maximum temperature in the case of the CCD cycle and positive in the case of the CD cycle. Accordingly, one would tend to assume that rafting occurs parallel to the stress axis for the CCD cycle and perpendicular to the stress axis for the CD cycle. However, the observation shows that the opposite is true. A closer inspection reveals that the microplastic strains observed (left side of Fig. 7) are positive (tensile) in the case of the CCD cycle and negative (compressive) in the case of the CD cycle. This observation illustrates not only the importance of plastic microstraining during rafting, as also evident from other studies,[3,4,6,11,14–16,37] but underlines in addition that the sign of the microstrains rather than just the sign of the stress determines the mode of raft formation.

Strength of rafted γ/γ' microstructure: dependence on stress and temperature

Rafting during high temperature deformation represents a dramatic change of the γ/γ' microstructure. In general, rafting occurs only at rather high temperatures above ~900°C, depending on the alloy. The question of obvious concern is whether and how rafting affects the high temperature strength. In the past, different criteria have been applied to assess the high temperature creep strength. For example, it has been a common practice to compare the minimum creep rates and/or creep rupture lives[4,7,15,20,38] of materials with either an initial cuboidal γ' structure or a rafted γ/γ' microstructure. From a practical point of view, knowledge of the creep rupture life is probably less useful than to know the time until a critical strain is attained. Such critical strains are generally of the order of <2%. The minimum creep rate is usually attained after similarly small strains. Hence, the minimum creep rate can usually be considered as a valid measure of the creep strength. In addition, other criteria may be useful to assess whether rafting is beneficial or detrimental to the creep strength. In particular, it is important to confine the discussion to specific ranges of temperature and stress.

The present knowledge can probably be condensed as follows. After the first reports, based on the effect of prerafting on creep rupture lives,[38] it was common belief that rafting improves the creep performance. The subsequent discussion became more differentiated and, at the same time, more controversial.[4,7,11,14,15,23,25,39,40] In many cases, it now appears justified to conclude that rafting will generally accelerate creep at higher stresses and retard creep at very low stresses,[7,14,15,20,25,40] as will be substantiated below. At the same time, as emphasised by Pollock's group,[4] caution is in place when generalising these statements to different kinds of superalloys and testing conditions. There seems to be agreement that the following criteria govern the deterioration or enhancement of the creep strength.[4,5,7,20,25,28,40,41] When the γ' phase is not circumvented but cut by dislocations, then this process accelerates the creep rate and leads to a deterioration, since the γ/γ' microstructure is coarsened at the same time. The other alternative, however, is that the γ' phase is not cut because the dislocations can circumvent the γ' phase by the glide/climb motion along the rather long γ/γ' interfaces, as envisaged by Carry and Strudel.[42] Then it is conceivable that, at low stresses and accordingly small strain rates, the climb component of the motion becomes the rate controlling mechanism and that rafting will retard creep. On the other hand, cutting of the γ' phase becomes the more probable process at higher stresses and strain rates (and/or lower temperatures).

In this and other respects, the important role of the interfacial dislocation networks that accompany the deformation process has been emphasised repeatedly.[3–6,10–17,20–24,26,28,29,33,41] On the one hand, the interfacial dislocation networks protect the γ' particles/plates,[5,10,43,44] while they also provide sources of dislocations for penetration of the γ' particles/plates,[5] once the accumulated internal stresses allow cutting of the γ' phase. In that latter case, the strength with which the γ' phase can resist cutting is one crucial factor which depends also on the nature and strength of the interfacial dislocation networks. More generally, as emphasised by Pollock and co-workers,[5,45] 'the balanced strength of the γ and γ' phases, the lattice misfit, and the interfacial networks must be addressed to control the creep resistance'. This emphasises that the alloying chemistry is of crucial importance and plays a complex role in the design of advanced Ni base superalloys.

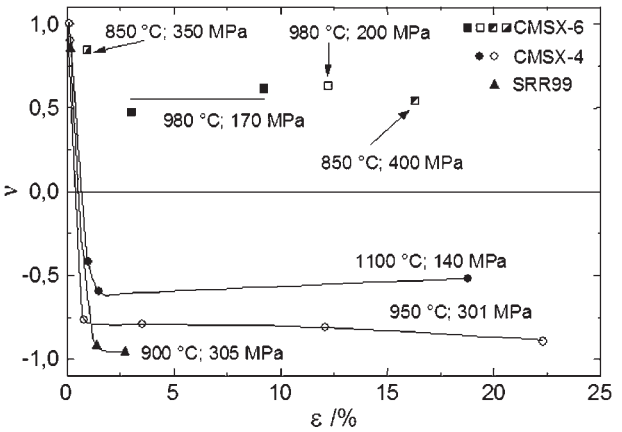

8 Plot showing development of connectivity, characterised by number ν, as function of creep strain under different testing conditions for different monocrystalline superalloys[15,46]

Cutting of γ' phase in rafted γ/γ' microstructures

Inversion of γ/γ' microstructure: role of connectivity

First, attention is drawn to the marked morphological change of the γ/γ' microstructure that occurs during rafting. As emphasised by Fredholm and Strudel,[26] it is found in many cases that, with progressing deformation and evolution of the rafts, the roles of γ and γ' phases undergo an inversion in the sense that in the end, the γ' phase encapsulates the γ phase and not vice versa. This inversion is not so surprising when it is considered that material transport by diffusion is bound to occur at high temperatures and that the γ' phase actually is the major phase. Fredholm and Strudel[26] have characterised the connectivity by a stereological parameter ν, with $\nu=1$ when the γ phase encapsulates the γ' phase and $-1<\nu<0$ in the opposite case. In Fig. 8, the evolution of the parameter ν with increasing plastic strain ε_{pl} is shown for different alloys (CMSX-6, CMSX-4 and SRR 99) and for different situations.[15,46] While the alloy CMSX-6 which has the smallest γ' volume fraction does not show significant inversion of the γ/γ' microstructure, the inversion is completed quickly within <2% of plastic strain in the alloys CMSX-4 and SRR 99. Figure 9 which will be discussed in more detail later shows schematically the processes of dislocation glide in the γ phase of a rafted microstructure.[40] The glide processes in the 'inverted' situation are sketched schematically (Fig. 9*b*) for comparison with the 'normal' initial situation (Fig. 9*a*). In the case of the extreme situation that the γ' phase completely encapsulates the γ phase, it is easily visualised that, with the onset of dislocation glide in the softer γ phase, interfacial dislocations will pile up at the γ/γ' interfaces and enhance the local stress in the γ' phase. Then, after a small deformation, further deformation can only proceed, if the γ' phase is cut. While complete inversion is improbable, it can still be concluded that γ' cutting will be favoured in those

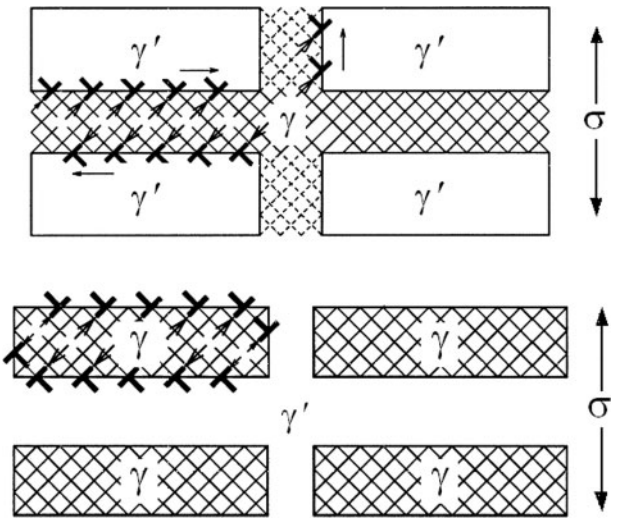

a γ' plates embedded in γ matrix; *b* after 'inversion', γ plates embedded in γ' 'matrix'

9 Schematic illustration of dislocation glide and accumulation of interfacial dislocations in rafted γ/γ' microstructures[15,40]

regions in which the γ/γ' morphology has been inverted and that the inversion of the connectivity during rafting will be one factor that leads to the deterioration of the high temperature strength.

Main factors that control γ' cutting

In a detailed study of the cutting of the γ' phase in the alloy CMSX-6 by dislocation pairs, Srinivasan *et al.*[47] came to the conclusion that this is a time dependent process involving diffusional mass transport between the two dislocations and could be rate controlling, once the γ' phase is cut. On the other hand, Pollock and co-workers[5,45] who studied ruthenium containing alloys concluded that in their alloys the most probable rate controlling mechanism was the time dependent 'climb of matrix dislocations into configurations that can shear the ordered high strength γ' rafts'. Irrespective of these differing views with respect to the rate controlling mechanism when the γ' phase is cut, a more detailed consideration of the dislocation processes at the γ/γ' interfaces is expedient in order to discuss more precisely whether and when the γ' phase is cut by dislocations.

Now, the processes sketched in Fig. 9 shall be discussed in more detail, referring to the two extreme situations that the γ' plates are either encapsulated by the γ phase as in the initial situation when the γ' particles are cuboidal (Fig. 9*a*) or that the γ' phase itself encapsulates the γ phase (Fig. 9*b*) (compare Refs. 15 and 40 for details). For the sake of simplicity, only two symmetrical glide systems of which only one is shown in the figure are considered to operate in the softer γ phase. In either case, dislocation glide will first be dominant in the horizontal γ channels (Fig. 9*a*) or γ plates (Fig. 9*b*) for the reasons discussed before, and the dislocations will accumulate at the horizontal γ/γ' interfaces. In the case sketched in Fig. 9*b*, it is evident that as the interfacial dislocation arrays become denser, deformation can only proceed if the γ' plates are cut. On the other hand, in the case shown in Fig. 9*a*, the dislocations can move by the Carry Strudel[42] glide climb process along the γ/γ' interfaces towards the edges of the γ' plates where they can escape by glide into the vertical γ channels. At the same time, as the back stress in the horizontal γ channels increases, more dislocation glide and deposition of dislocations can possibly occur also in the small remaining vertical γ channels. In the rafted microstructure, the processes at the much longer horizontal γ/γ' interfaces are considered to dominate the behaviour. Aside from that, there is one fundamental difference between the nature of the interfacial dislocations that accumulate at the horizontal and at the vertical γ/γ' interfaces in either of the two cases shown in Fig. 9. While the former relieve the coherency stresses and, beyond a certain stage, build up stresses in the opposite sense, the latter dislocations will in fact reinforce the original coherency stresses. Coming to the question of cutting of the γ' plates, it must be noted that while the interfacial dislocation arrays at the horizontal γ/γ' interfaces will introduce transverse compressive stresses in the γ' plates, those at the vertical γ/γ' interfaces will lead to increasing tensile stresses in the γ' plates. Thus, both types of deformation induced internal stresses will aid deformation of the γ' phase. When the deformation induced internal stresses in the γ' plates have become large enough, the γ' plates will ultimately be cut by the dislocations. It is hence obvious that the density of deformation induced interfacial dislocations is suitable to provide information on the strength of the γ' plates. Such considerations have led the group of Pollock to investigate in some detail the formation of interfacial dislocation networks in alloys of different compositions and lattice misfit with the aim to assess quantitatively to what extent the interfacial networks were denser than the equilibrium networks that would exactly compensate the original γ/γ' lattice misfit.[4,45] The density of the 'excess' interfacial dislocations can then be considered as an indicator of the resistance of the γ' phase against cutting.

Simplified 2D model of cutting of γ' plates of rafted microstructure

The precise computation of the formation of the interfacial dislocation networks and the subsequent cutting of the γ' phase is a formidable 3D multiscale problem. Here, the author shall confine himself to discuss the results of a very simple 2D model in which only two symmetrically operating glide systems are considered. Details of the model are presented in the section on 'Appendix'. The model considers only athermal stresses and takes into account the coherency stresses and the deformation induced internal stresses which stem from the dislocation networks and the latter's resistance against glide dislocations entering the γ' plates. The model, as sketched in Fig. 10, considers only stresses in the plane of Fig. 10 and only athermal glide mechanisms. For the simplified situation considered, the condition for the cutting of the γ' plates of the rafted microstructure, based on the Tresca shear stress criterion, has been derived as follows

$$\sigma_{\text{ext}} \geqslant 2\tau_{0,\gamma'} + 2\alpha G_{\gamma'} bn - f_{\gamma} E_{\gamma'} nb \qquad (2)$$

where σ_{ext} is the external tensile stress (acting in the vertical direction), $\tau_{0,\gamma'}$ is the shear stress required to cut the γ' plates for whatever mechanism my be operative, $G_{\gamma'}$ is the shear modulus of the γ' phase, b is

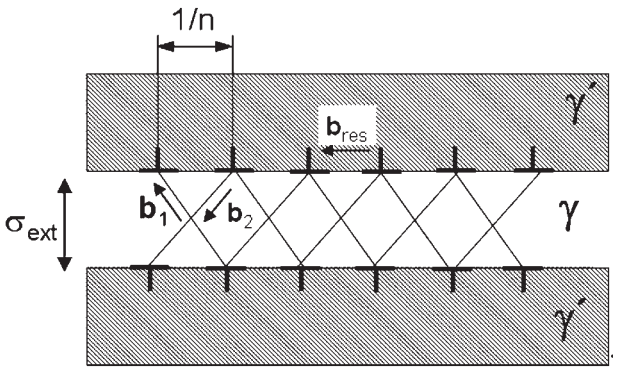

10 Schematic 2D view of tensile deformation of horizontal γ layer of rafted γ/γ' microstructure by glide of dislocations with Burgers vectors b_1 and b_2 of two symmetrically operating slip systems: sketched dislocations at γ/γ' interfaces are 'resultant' dislocations with resultant Burgers vector b_{res} which lies parallel to γ/γ' interface

the modulus of the Burgers vector , α is a geometric constant, f_γ is the volume fraction of the γ phase, E_γ is the Young's modulus of the γ phase (assumed to be roughly the same as the Young's modulus $E_{\gamma'}$ of the γ' phase) and n is the line density of interfacial dislocations at the horizontal γ/γ' interface which would be related to the spacing l between the interfacial dislocations as $l=1/n$. The criterion for cutting of the γ' plates can be formulated alternatively in terms of the line density n of the interfacial dislocations that are required to build up the necessary stress

$$n \geqslant \frac{2\tau_{0,\gamma'} - \sigma_{ext}}{f_\gamma E_{\gamma'} b - 2\alpha G_{\gamma'} b} \quad (3)$$

In the above equations, the lattice misfit δ does not appear explicitly for the reasons stated below and in the section on 'Appendix'.

While the model on which these relations were based is crude, it is transparent and provides quick insight into the terms that govern the cutting of the γ' plates. Briefly speaking, in the present approximation, the tensile stress that must be applied so that the γ' plates are cut by the dislocations consists of three contributions, namely the shear strength $\tau_{0,\gamma'}$ of the γ' plates, the 'Orowan type' bowing stress $\alpha G_{\gamma'} bn = \alpha G_{\gamma'} b/l$ that must be applied to allow the dislocations to overcome the interfacial network and the deformation induced internal transverse compressive stress $E_{\gamma'} f_\gamma nb$ which arises from the dislocation networks and supports tensile deformation of the γ' plates. The transverse tensile coherency stress $E_{\gamma'} f_\gamma \delta$ in the γ' plates cancels precisely in the expression for the tensile stress, if the longitudinal coherency stress in the γ' plates in the direction of the external stress is assumed to be exactly of the same magnitude, i.e. $E_{\gamma'} f_\gamma \delta$ (compare the section on 'Appendix' for further details). In order to estimate the relative importance of the contribution from dislocation glide through the dislocation networks, the relative magnitudes of the terms $\alpha G_{\gamma'} b$ and $f_\gamma E_{\gamma'} b$ (which determine the sign of the denominator in equation (3)) should be compared. Inserting typical values for f_γ ($\sim$0·3) and $G_{\gamma'}$ and $E_{\gamma'}$, it follows that $\alpha G_{\gamma'} b > f_\gamma E_{\gamma'} b$. This means that the extra stress that is necessary to overcome the dislocation network is larger than the stress reduction due to the deformation induced internal forward stresses that aid the cutting of the γ' plates. Hence the denominator in equation (3) is negative, just like the numerator (so that $n>0$), but significantly smaller than it would be, if the stress for overcoming the dislocation network were neglected. In that case, the term $\alpha G_{\gamma'} b$ disappears in both equations, and then the line density n, beyond which γ' cutting would occur, becomes smaller. On the other hand, when the resistance of the dislocation network against dislocation glide into the γ' plates is taken into account, an accordingly larger line density n of the interfacial dislocations must be accumulated before cutting of the γ' plates can occur. Then, according to equation (2), the γ' plates would become more resistant against the applied stress, as emphasised by Harada's group.[17,43,44] The above dislocation model can of course convey only a semiquantitative understanding of the factors that control cutting of the γ' plates. A quantitative assessment would require a more detailed rigorous 3D treatment.

Is there an optimum γ/γ' lattice misfit?

Since the γ/γ' lattice misfit has frequently been considered to be one of the important metallurgical factors that control the high temperature strength of nickel base superalloys, it is appropriate to pose the question whether there exists an optimum γ/γ' lattice misfit. In the literature, widely different views have been voiced such as, for example:

(i) the γ/γ' lattice misfit should be as small as possible in order to avoid coarsening[5]

(ii) the γ/γ' lattice misfit should be large so that dense dislocation networks form on the γ/γ' interfaces. These networks would then protect the γ' phase against cutting by dislocations and would thereby improve the high temperature strength. One prediction of this approach is that the spacings between the dislocations in the interfacial networks should be proportional to the minimum creep rate.[17,43,44]

In practice, some experimental facts are found in support of either statement, while others contradict either statement. For example, empirically, it is found that a material with good high temperature creep resistance will usually have a rather large negative lattice misfit.[4,10,14,43–45] On the other hand, it has been found that, in ruthenium containing superalloys of rather high misfit in which very dense interfacial dislocation networks developed, 'the difference in dislocation spacing does not seem to have strong influence on overall creep rupture life in present study'[48] or that 'in this set of alloys the creep rates do not directly scale with the magnitude of the misfit'.[45] In another study on ruthenium bearing superalloys, Rowland *et al.*[49] concluded that 'the most obvious factor influencing creep strength in the alloys studied here is the volume fraction of γ''. It must be concluded that, while there can be no doubt that the interfacial networks add to the deformation resistance of the γ' plates, this fact is only one of the factors that govern the high temperature strength of superalloys. Probably, some of the uncertainties could be eliminated or reduced, if the creep resistance were defined less globally but more specifically for each given alloy and for a particular limited range of temperature and stress.

The γ/γ' lattice misfit can only be varied by changing the alloy chemistry. However, by changing the alloy chemistry, all other composition dependent properties of the alloy are also changed so that it becomes difficult if not impossible to single out the effect of the change in lattice misfit on the mechanical properties. In view of these difficulties to ascertain the influence of the lattice misfit on the creep resistance, the author considers a theoretical approach by Svoboda and Lukáš[50,51] very interesting. These authors developed a rather detailed dislocation model of the creep deformation for different stresses at both 'high' and 'low' temperatures. In their model, they attempted to include most of the experimentally observed details. Then, keeping all other parameters constant, they could vary the lattice misfit parameter δ and see how this affected the creep curves. The author's confidence in the work of Svoboda and Lukáš is based mainly on the fact that they were able to reproduce very satisfactorily for the alloy CMSX-4 the rather complex shapes of the creep curves in the $\dot{\varepsilon}_{pl}$ versus ε_{pl} plots (compare Fig. 5) which are very sensitive to small variations of the creep behaviour. The following results are noteworthy. At a 'high' temperature of 1000°C, the results of the modelling suggest that a low magnitude of the misfit parameter δ would be favourable to reduce in particular the initially high creep rate. In contrast, it was found that at a 'low' temperature of 750°C the rather high creep rate in what the authors called the 'quick creep' regime would be lowered significantly, when the magnitude of the misfit parameter δ was larger. Hence, they concluded that a superalloy that would exhibit good creep resistance at both 'low' and 'high' temperatures should have a misfit parameter with a rather high magnitude at 'low' temperatures and a rather low magnitude at 'high' temperatures. However, the temperature dependence of the lattice spacings a_γ and $a_{\gamma'}$ is such that, in alloys with negative lattice misfit, the latter becomes more negative (i.e. increases in magnitude) above ~600°C, because the expansion of the γ phase increases more strongly than that of the γ' phase above ~600°C.[52,53] Thus, it would be impossible to design an alloy which would have a good creep resistance at both 'low' and 'high' temperatures. This led Svoboda and Lukáš to conclude, 'The results of the modelling indicate that the value of δ for the alloy CMSX-4 is not suitable, namely $|\delta|$ is small at low temperatures and high at high temperatures. If it were just the opposite, the creep properties would be – according to the theoretical prediction – much better'.

This conclusion motivates the idea that the requirements postulated by Svoboda and Lukáš could perhaps be fulfilled better by an alloy with a positive lattice misfit.[6] If the temperature dependence of the lattice spacings a_γ and $a_{\gamma'}$ remained similar as before, then a positive lattice misfit of appreciable magnitude at the lower temperature would become smaller in magnitude at a higher temperature. The data on superalloys with positive lattice misfit are very limited and do not suggest, at least for the alloys so far studied, that these alloys have superior creep properties.[49] This is disappointing but not surprising, because the alloying chemistry affects not only the lattice misfit but also other properties which control the overall strength. Therefore, the requirement of a positive lattice misfit should be coupled with the additional condition that all other properties of the γ and γ' phases should remain more or less unchanged so that the benefit from the positive lattice mismatch would not be outweighed by negative consequences with respect to other important material properties. Assuming that an alloying chemistry that matches these requirements could be found, a number of other positive effects, which would make a positive lattice mismatch attractive, are to be expected with respect to creep and fatigue strength. These additional beneficial effects will be detailed subsequently.

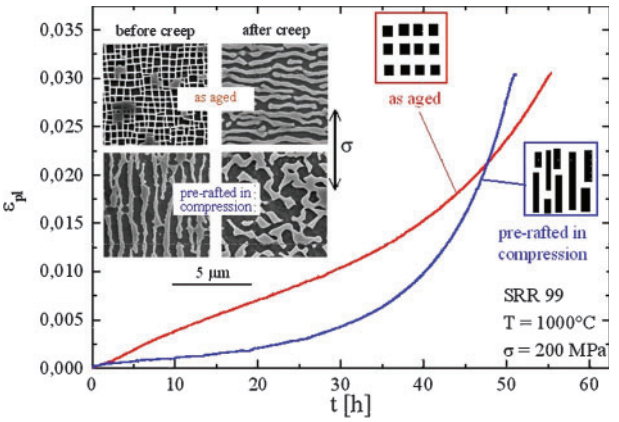

11 Comparison of tensile creep behaviours of single crystals of the superalloy SRR 99 with initial as aged γ/γ' microstructure and with initial γ/γ' microstructure prerafted in compression: insets show initial microstructures before and after creep for both cases[54]

Enhancement of tensile creep and fatigue performance by prerafting in compression

In detailed studies on the superalloys CMSX-6 and CMSX-4, an attempt was made to exploit rafting as a means to improve the high temperature creep and fatigue strength by prior introduction of rafts parallel to the stress axis by a small defined compressive creep deformation.[54,55] The idea behind these studies was simple. With respect to high temperature creep, it follows from dislocation mechanics that the dislocation glide climb motion along vertical γ/γ' interfaces is considerably slower than along horizontal γ/γ' interfaces.[54] This fact suggested that in the regime in which the glide climb motion is rate controlling, rafts parallel to the stress axis would retard creep. In the case of fatigue, it was to be expected that the propagation of fatigue cracks would be hindered by γ' rafts lying parallel to the stress axis, whereas crack growth along rafts lying perpendicular to the stress axis would be easier. These expectations were fully borne out in the experiments which will be discussed in the following.

An example of the beneficial effects of prerafting in compression on the tensile creep behaviour is shown in Fig. 11. In the plot, tensile creep curves (ε_{pl} versus time t) at 1000°C of two specimens of the superalloy SRR 99 are compared. One specimen had been tested in the standard heat treated state with initial cuboidal γ' particles, the other specimen had been creep deformed before the tensile creep test by $<0{\cdot}4\%$ strain in compression and contained well developed rafts parallel to the stress axis as the initial γ/γ' microstructure. It is clearly seen that the initial creep deformation proceeds much more slowly in the prerafted specimen than in the specimen with the cuboidal γ' particle microstructure.

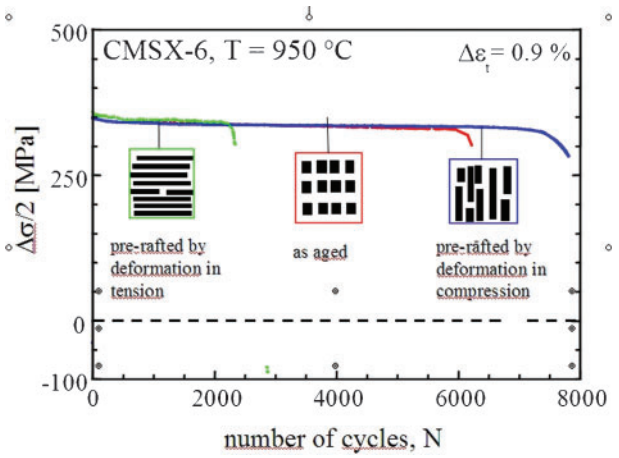

12 Comparison of cyclic deformation curves (stress amplitude $\Delta\sigma/2$ versus number of cycles N) of single crystals of superalloy CMSX-6 with three different initial γ/γ' microstructures (as aged, prerafted in tension, prerafted in compression): cyclic deformation was performed in strain control at total strain amplitude $\Delta\varepsilon_t/2=0{\cdot}9\%$ (Ref. 55)

However, at a strain of ~2%, the two creep curves intersect, and the prerafted specimen then deforms more rapidly than the specimen with the initial cuboidal γ' particle microstructure. This behaviour is easily explained when one inspects the γ/γ' microstructures in both specimens (see inset) before and after the creep test. In the case of the initial cuboidal γ' particles, the microstructure undergoes rafting perpendicular to the stress axis as expected. On the other hand, in the prerafted specimen, the rafts have the 'wrong' orientation for tensile creep, and therefore become unstable and are transformed during the first 2% of plastic strain into an unspecific γ/γ' microstructure which is less creep resistant than the rafted microstructure in the other specimen. Nonetheless, since only small creep strains are tolerated in practice, prerafting in compression does offer an advantage which would of course be much bigger, if one succeeded in stabilising the raft structure parallel to the stress axis. Quite recently, Shui *et al.*[56,57] have reported results of similar studies in which they verified the findings of Tetzlaff and Mughrabi[54] and obtained in addition other interesting results.

In related tests, the high temperature cyclic deformation and fatigue behaviours of specimens of the monocrystalline superalloys CMSX-4 and CMSX-6 with different initial γ/γ' microstructures were compared in strain controlled tests.[55] As an example, Fig. 12 shows cyclic hardening curves (stress amplitude $\Delta\sigma/2$ versus number of cycles N) of specimens of the alloy CMSX-6 with three different initial γ/γ' microstructures, namely cuboidal γ' particles and γ/γ' rafts lying either perpendicular or parallel to the stress axis. The rafts had been introduced by a (very) small prior creep deformation in either tension or compression, respectively. As expected, the specimen with the rafts lying parallel to the stress axis exhibited the longest fatigue life, whereas the specimen with the rafts orientated perpendicular to the stress axis failed after the smallest number of cycles. The fatigue life of the specimen with the cuboidal γ' particles was intermediate between the two extremes. The SEM micrographs showed that when the rafts were orientated perpendicularly to the stress axis, the cracks propagated along a smooth fracture surface through the γ phase or along the γ/γ' interfaces. On the other hand, when the rafts were parallel to the stress axis, they obstructed crack growth and induced crack branching, as the cracks tried to circumvent the γ' rafts. An intermediate mode of crack growth was observed in specimens with the initial γ/γ' microstructure with cuboidal γ' particles. The results obtained on specimens of the superalloy CMSX-4 were qualitatively similar.[55]

Since thermomechanical fatigue CCD cycles, with upper and lower temperatures of ~1100 and ~600°C respectively, are considered as a most damaging loading mode at the leading edge of turbine blades during start-up and shut-down operation, the TMF behaviours of specimens of the alloy SRR 99 with different initial γ/γ' microstructures were also investigated.[56] The most important result was, as in the case of isothermal fatigue, that prerafting in compression induced crack branching and thereby improved TMF life.

These experiments verify that rafts lying parallel to the stress axis can be beneficial for tensile creep and, at the same time, for both isothermal and thermomechanical fatigue at high temperatures. As far as the creep performance is concerned, it follows that, if a superalloy could be designed that had not only good high temperature strength but, at the same time, a positive lattice misfit, it should have a superior high temperature creep behaviour, because rafting would occur parallel to the stress axis and retard creep deformation at high temperatures. It could also be speculated that the same alloy would exhibit very good TMF resistance during CCD cycling, since rafts would be expected to develop parallel and not perpendicular to the stress axis, as would normally be the case for an alloy with negative lattice misfit (compare Fig. 6).

In the context of trying to exploit the advantages of rafts lying parallel to the stress axis, some recent work in Harada's group is of interest. Murakumo *et al.*[57] studied a model monocrystalline superalloy with a designated high γ' volume fraction of 80%. In this alloy, the γ phase was dispersed in the γ' phase which then assumes the role of the matrix. After tensile creep testing at 1100°C, it was found that rafting had occurred parallel to the stress axis. This was surprising in view of the fact that the lattice misfit of the alloy was negative. The authors explained their observation by pointing out that exchanging the roles of the γ and γ' phases is equivalent to changing the lattice misfit from negative to positive. It appears worthwhile to follow these ideas in more detail in the hope that suitable measures can be derived to obtain enhanced creep and fatigue strengths.

Alloying effects: interplay between driving force for coarsening and diffusion kinetics

More recently developed superalloys frequently contain higher amounts of refractory elements such as rhenium and, more recently, also ruthenium/iridium additions. These alloying elements affect the properties in different ways, providing for example strong solid solution hardening of the γ phase and good microstructural

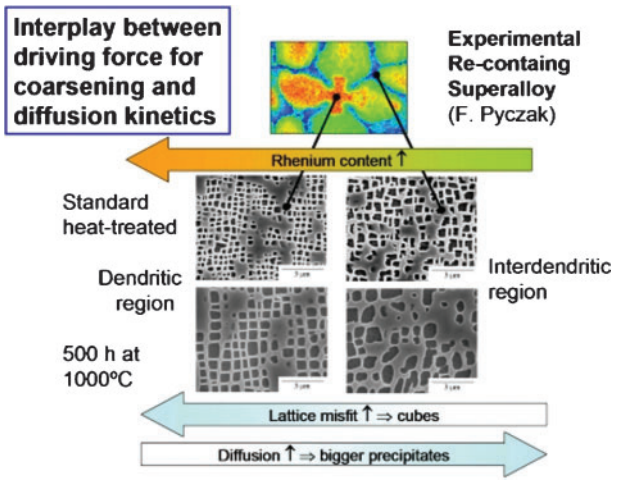

13 Schematic illustration of interplay of driving force for coarsening and diffusion kinetics in rhenium containing superalloy: effects of increasing rhenium content on lattice misfit and on rate of diffusion are indicated; micrographs refer to situations for as aged condition and after annealing treatment in dendritic and in interdendritic regions (compare also Ref. 58)

stability. At the same time, they affect the γ/γ' lattice misfit and the kinetics of diffusion, modifying both the tendency for coarsening and the kinetics of coarsening. Thus, interesting effects can come about. Here, this is illustrated schematically in Fig. 13 for the case of an experimental rhenium containing superalloy[58] which was studied in the standard heat treated state and after a 500 h anneal at 1000°C. In this alloy, the rhenium content was found to be larger in the dendritic than in the interdendritic regions. The annealing treatment led to a noticeable more or less isotropic coarsening of the γ' particles in both dendritic and interdendritic regions. The precipitate growth was found to be larger in the interdendritic than in the dendritic regions. This observation seems surprising since rhenium is known to increase the magnitude of the lattice misfit, as has been studied in detail by Pyczak *et al.*[59] Hence, the driving force for coarsening is expected to be increased. However, this effect is counteracted by the slowing down of the diffusion kinetics by the addition of rhenium.[58,60] Thus, the competition between the enhancement of the driving force for coarsening and the slowing down of the diffusion kinetics by the addition of rhenium becomes decisive. In the present case, the latter effect apparently outweighed the former effect. This result becomes even more interesting in the light of the finding that, in creep tests on the same specimens, more pronounced rafting occurred in the dendritic than in the interdendritic regions. Again, this is a surprising finding which can be taken as an indication that, in the present case, the driving force for rafting is so markedly enhanced by the increased magnitude of the lattice misfit in the dendritic regions (and by the stress gradient that develops between the horizontal and the vertical channels when an external stress is applied)[15,16,22] that the reduced rate of diffusion is more than compensated. The important conclusion is that, 'at a given temperature, the same alloying element can impede undirectional (i.e. isotropic) coarsening in the absence of an applied stress but promote the process of directional coarsening during deformation'.[58]

Summary and conclusions

Is there an optimum design strategy to develop superior nickel base superalloys?

The present knowledge on superalloys and on the microstructural features that govern their high temperature strength is based on the results of immense research efforts over the last decades. The ongoing endeavours to achieve further progress are documented by more recent studies which deal, for example, with new concepts of alloy development[61,62] or more subtle details of how dislocation glide and diffusion processes act in combination during deformation at high temperatures[63] or detailed dislocation modelling of the stability of interface dislocation configurations.[64] Ultimately and aside from the more academic questions, the progress achieved must gradually merge into further improvements of the properties of superalloys.

In this context, it must be emphasised that the preceding discussion has addressed only a limited number of the more important microstructural aspects of the high temperature strength of monocrystalline nickel base superalloys. Still, these considerations show that, in striving for superalloys with improved superior high temperature strength properties, it is imperative to consider a larger number of important features and properties at the same time. It is also clear that in many cases a price has to be paid for the improvement of a particular property, since the alloying measures taken will frequently lead to a deterioration of another property. This is best illustrated by the following summary which lists examples of some properties that are generally recognised as desirable and important but difficult to achieve at the same time.

1. High γ' volume fraction: desirable but promotes inversion of γ/γ' microstructure during creep and thus cutting of γ' phase.
2. Strong solid solution hardening of γ phase: desirable and achievable by alloying with (refractory) elements. However, this can lead to unpredictable effects on lattice misfit, diffusion kinetics and formation of topologically close packed phases.
3. Low driving force for coarsening: desirable, would require small lattice mismatch δ (at the high temperature of operation) which is rarely found in current commercial alloys.
4. High lattice mismatch δ and driving force for coarsening: this alternative would follow some opinions that rafting is generally beneficial, contrary to some other opinions.
5. Rafting parallel to the stress axis in tensile creep: this would enhance tensile creep and thermomechanical fatigue strengths, and would require a positive lattice misfit $\delta>0$. However, at present, commercial alloys all have negative lattice misfit $\delta<0$, and current alloys with $\delta>0$ do not combine this with good high temperature strength properties.
6. Optimised creep strength at both low and high temperatures: this would also require a positive lattice misfit $\delta>0$ with the problems listed above.
7. Microstructural stability: this would be favoured by small magnitude of lattice misfit and slow diffusion

kinetics. The latter is achievable by alloying, but could enhance the lattice misfit δ and hence the driving force for coarsening.

It is obvious that there exist substantial discrepancies between the requirements with respect to one particular desirable property and the negative side effects on other important properties. The conclusion is that the optimum design of superior superalloys can only be based on intelligent compromises between the listed design criteria.

Appendix

Simplified 2D model of cutting of γ' plates during tensile deformation of rafted γ/γ' microstructure

The dislocation model is sketched in Fig. 10. For the sake of simplicity, the rafted plates are treated as though they were infinitely long. In other words, dislocation glide in the vertical γ channels or interfacial dislocation networks at the vertical γ/γ' interfaces are not explicitly considered. The deformation induced interfacial dislocations of the two symmetrically operating slip systems are represented by 'resultant' dislocations with a resultant Burgers vector b_{res} formed by vectorial combination of the Burgers vectors of pairs of dislocations from the two slip systems. Before entering the mathematical formulation, it is emphasised that the main aim of the following derivations is to provide only a semiquantitative understanding of the roles played by the different stress contributions that govern the cutting of the γ' plates. Hence, no effort has been made to express the used numerical (geometric) constants accurately.

The line density of the interfacial dislocations is denoted by n, implying that $1/n$ is the spacing between resultant interfacial dislocations. Inspection of the interfacial dislocations makes it evident that they introduce lateral internal compressive stresses in the γ' plates. These internal compressive stresses superimpose on the externally applied tensile stress σ_{ext} and on the initially present coherency stresses $\Delta\sigma_{\gamma'}^{\mathrm{coh}}$ and aid the tensile deformation of the γ' plates. The dense interfacial dislocation networks represent an obstacle against glide into the γ' plates[5,43,44] which can only be overcome, if glide dislocations or interfacial dislocation segments of length $l = 1/n$ bow out between two neighbouring interfacial dislocations. It is assumed that this bowing stress is of the form $\alpha G_{\gamma'} b/l = \alpha G_{\gamma'} bn$, where $G_{\gamma'}$ is the shear modulus in the γ' phase and α a constant that depends on the strength of the junctions of the network and that should lie in the range $0{\cdot}5 < \alpha < 1$. In the end, the sum of all the stress contributions named must be large enough to overcome the shear strength $\tau_{0,\gamma'}$ of the γ' plates. Microscopic details of the cutting mechanism are not considered but lumped into the quantity $\tau_{0,\gamma'}$.

The initial coherency stresses in the γ' phase are triaxial tensile stresses $\Delta\sigma_{\gamma'}^{\mathrm{coh}}$. It is easily shown that the magnitude of these coherency stresses can be expressed approximately as

$$\Delta\sigma_{\gamma'}^{\mathrm{coh}} = -\frac{f_\gamma E_\gamma \delta}{f_{\gamma'} E_{\gamma'} + f_\gamma E_\gamma (1-\delta)} E_{\gamma'} \approx -f_\gamma \delta E_{\gamma'} \approx +f_\gamma n_{\mathrm{equi}} b E_{\gamma'} \quad (4)$$

where f_γ and $f_{\gamma'}$ are the volume fractions and E_γ and $E_{\gamma'}$ the Young's moduli of the γ and γ' phases respectively, and δ is the lattice misfit parameter (compare equation (1)). The strongly simplified form on the right hand side is obtained with the approximation $(1-\delta) \approx 1$ and $E_\gamma \approx E_{\gamma'}$. In this approximate expression, the lattice misfit δ has been replaced by the equivalent expression $n_{\mathrm{equi}} b$ (Brooke's formula, the minus sign is chosen for negative δ), where n_{equi} represents the equilibrium line density of interfacial dislocations that would just be necessary to compensate the initial coherency stress. Thus, in the initial state, tensile coherency stresses of the form described above prevail in the γ' plates in both the vertical and the lateral (horizontal) directions. The former superimpose on the external tensile stress σ_{ext} and reinforce it, while the latter impede tensile deformation. However, because these tensile coherency stresses have the same magnitude and act perpendicularly to each other, they do not contribute to the shear stress.

It follows from Fig. 10 that the interface dislocations at the horizontal γ/γ' interfaces introduce lateral deformation induced internal compressive stresses in the γ' plates. These compressive stresses act against the lateral tensile coherency stresses and can be expressed approximately as

$$\Delta\sigma_{\gamma'}^{\mathrm{def}} = -\frac{f_\gamma E_\gamma n b_{\mathrm{res}}}{f_{\gamma'} E_{\gamma'} + f_\gamma E_\gamma (1 + n b_{\mathrm{res}})} E_{\gamma'} \approx -f_\gamma n b_{\mathrm{res}} E_{\gamma'} \quad (5)$$

The strongly simplified form on the right hand side obtains with the approximations $E_\gamma \approx E_{\gamma'}$ and $(1 + n b_{\mathrm{res}}) \approx 1$. Cutting of the γ' plates becomes possible, when the overall shear stress $\tau_{\gamma'}$ that acts in the γ' plates is large enough to overcome their shear strength $\tau_{0,\gamma'}$, which will of course depend on the cutting mechanism that is operative. For the present semiquantitative approach and for the sake of simplicity, this overall shear stress is not expressed for a particular crystallographic constellation but as a Tresca shear stress

$$\tau_{\gamma'} = \frac{\sigma_{\mathrm{ext}} - f_\gamma \delta E_{\gamma'} - (-f_\gamma \delta E_{\gamma'} - f_\gamma n b_{\mathrm{res}} E_{\gamma'})}{2} \approx \frac{\sigma_{\mathrm{ext}} + f_\gamma n b_{\mathrm{res}} E_{\gamma'}}{2} \quad (6)$$

In this formulation, it was assumed that the vertical coherency stresses in the γ' plates have the initial magnitude given by equation (4), based on the assumption that dislocation glide in the vertical γ channels has been so limited, that the original tensile coherency stresses remain unaffected, as supported by some observations.[10] It should be noted that in this case the terms with the misfit parameter δ cancel, leading to the simplified expression on the right. If stronger dislocation glide had occurred in the vertical γ channels, then the superposition of additional tensile deformation induced internal stresses on the initial coherency stresses in the γ' plates would have to be considered, and the shear stress $\tau_{\gamma'}$ would become accordingly larger. Now, considering in addition the shear stress $\alpha G_{\gamma'} bn$ (compare section on 'Simplified 2D model of cutting of γ' plates of rafted microstructure') that is necessary to overcome the glide resistance of the interfacial dislocation network, the cutting condition can be formulated as

$$\sigma_{ext} \geqslant 2\tau_{0,\gamma'} + 2\alpha G_{\gamma'} bn + f_\gamma E_{\gamma'} \delta - f_\gamma E_{\gamma'} (\delta + nb_{res})$$
$$\approx 2\tau_{0,\gamma'} + 2\alpha G_{\gamma'} bn - f_\gamma E_{\gamma'} bn \quad (7)$$

Again, it should be noted that the terms containing the misfit parameter δ cancel. In the further simplified expression on the right, the (small) difference between the magnitudes of the Burgers vectors b and b_{res} has been ignored. Alternatively, equation (7) can be resolved for the line density n

$$n \geqslant \frac{2\tau_{0,\gamma'} - \sigma_{ext}}{f_\gamma E_{\gamma'} b - 2\alpha G_{\gamma'} b} \quad (8)$$

Finally, two details are pointed out:

(i) it is noted that if the tensile coherency stress in the γ' plates that superimposes on the external tensile stress σ_{ext} were neglected, then the term with the misfit parameter δ would appear again, δ could be replaced by the equivalent expression $n_{equi}b$ and the equation (7) could be formulated in terms of the line density ($n - n_{equi}$) of what Pollock *et al.*[4,45] call the 'excess interfacial dislocations'. However, there appears to be no convincing physical reason in favour of this approximation. Nonetheless, the quantity (n–n_{equi}) can of course still be calculated by subtracting $n_{equi} = -\delta/b$ from n, as expressed by equation (8)

(ii) if the resistance of the interfacial dislocation network to deformation of the γ' plates were neglected, then all terms containing $\alpha G_{\gamma'} b$ would disappear in the above expressions, and γ' cutting could occur at a correspondingly smaller line density n of interfacial dislocations.

Acknowledgements

The author expresses his appreciation to the Diplom and Doctoral students who contributed over the years to the work presented in this review. He thanks Florian Pyczak and Steffen Neumeier for a critical reading of the manuscript and for fruitful discussions. Much of the work reported was funded by the Deutsche Forschungsgemeinschaft and by the German Ministry of Science and Education. This support is acknowledged gratefully.

References

1. M. Gell, D. N. Guhl, D. K. Gupta and K. D. Sheffler: *Mater. Sci. Technol.*, 1987, **39**, 11–15.
2. G. L. Erickson: Proc. 8th Int. Symp. on 'Superalloys', (ed. R. D. Kissinger *et al.*), 35–44; 1996, Warrendale, PA, The Minerals, Metals and Materials Society.
3. J.-L. Strudel: in 'Physical metallurgy', (ed. R. W. Cahn and P. Haasen), Vol. 3, 2105–2206; 1996, Amsterdam, Elsevier Science BV.
4. T. M. Pollock and R. D. Field: in 'Dislocations in solids', (ed. F. R. N. Nabarro and M. S. Duesberry), Vol. 11, 547–618; 2002, Amsterdam, Elsevier Science BV.
5. R. C. Reed: 'The superalloys, fundamentals and applications', 120–216; 2006, Cambridge, Cambridge University Press.
6. H. Mughrabi and U. Tetzlaff: *Adv. Eng. Mater.*, 2000, **2**, 319–326.
7. P. Caron, P. J. Henderson, T. Khan and M. McLean: *Scr. Metall.*, 1986, **20**, 875–880.
8. P. J. Henderson and M. McLean: *Scr. Metall.*, 1985, **19**, 99–104.
9. M. McLean: *Philos. Trans. Roy. Soc. Lond. A*, 1995, **351A**, 419–433.
10. T. P. Gabb, S. L. Draper, D. R. Hull, R. A. MacKay and M. V. Nathal: *Mater. Sci. Eng. A*, 1989, **A118**, 59–69.
11. T. M. Pollock and A. S. Argon: *Acta Metall.*, 1994, **42**, 1859–1874.
12. J. Y. Buffière and M. Ignat: *Acta Metall. Mater.*, 1995, **43**, 1791–1797.
13. H.-A. Kuhn, H. Biermann, T. Ungár and H. Mughrabi: *Acta Metall. Mater.*, 1991, **39**, 2783–2794.
14. F. R. N. Nabarro: *Metall. Mater. Trans. A*, 1996, **27A**, 513–530.
15. H. Mughrabi: Proc The Johannes Weertman Symp., (ed. R. J. Arsenault *et al.*), 267–278; 1996, Warrendale, PA, The Minerals, Metals and Materials Society.
16. M. Véron, Y. Bréchet and F. Louchet: *Acta Metall. Mater.*, 1996, **44**, 3633–3641.
17. T. Link and M. Feller-Kniepmeier: *Z. Metall.*, 1987, **78**, 617–621.
18. S. Reichstein: 'Diplomarbeit'; 1996, Erlangen, Universität Erlangen-Nürnberg.
19. S. Reichstein, S. Kraft and H. Mughrabi: submitted to *Intern. J. Mater. Res*, 1996.
20. M. V. Nathal, R. A. McKay and R. V. Miner: *Metall. Trans. A*, 1989, **20A**, 133–141.
21. M. Feller-Kniepmeier and T. Link: *Metall. Trans. A*, 1989, **20A**, 1233–1238.
22. T. M. Pollock and A. S. Argon: *Acta Metall.*, 1992, **40**, 1–30.
23. B. Fedelich: Personal communication, 1999.
24. P. Caron and T. Khan: *Mater. Sci. Eng. A*, 1983, **A61**, 173–184.
25. R. A. MacKay and L. J. Ebert: *Metall. Trans. A*, 1985, **16A**, 1969–1982.
26. A. Fredholm and J.-L. Strudel: in 'High temperature alloys, their exploitable potential', (ed. J. B. Marriott *et al.*), 9–18; 1987, London and New York, Elsevier Applied Science.
27. W. Schneider, J. Hammer and H. Mughrabi: Proc. 7th Int. Symp. on 'Superalloys'' (ed. S. D. Antolovich *et al.*), 589–598; 1992, Warrendale, PA, The Minerals, Metals and Materials Society.
28. H. Mughrabi, W. Schneider, V. Sass and C. Lang: Proc. 10th Int. Conf. on 'Strength of materials', (ed. H. Oikawa *et al.*), 705–708; 1994, Sendai, The Japan Institute of Metals.
29. N. Matan, D. C. Cox, C. M. F. Rae and R. C. Reed: *Acta Mater.*, 1999, **47**, 2031–2045.
30. S. Draper, D. Hull and R. Dreshfield: *Metall. Trans. A*, 1989, **20A**, 683–688.
31. H. Biermann, S. Spangel and H. Mughrabi: *Z. Metall.*, 1996, **87**, 403–410.
32. B. von Grossmann, H. Biermann, S. Mechsner and H. Mughrabi: Proc. 6th Liège Conf. on 'Materials for advanced power engineering', (ed. J. Lecomte-Beckers *et al.*), Vol. 5, No. 3, 1429–1438; 1998, Jülich GmbH, Forschungszentrum Jülich.
33. W. Schneider: Dr.-Ing. Thesis, Hochtemperaturkriechverhalten und Mikrostruktur der einkristallinen Nickelbasis–Superlegierung CMSX-4 bei Temperaturen von 800°C bis 1100°C, 1993, Universität Erlangen-Nürnberg.
34. W. Schneider and H. Mughrabi: Proc. 5th Int. Conf. on 'Creep and fracture of engineering materials and structures', (ed. B. Wilshire and R. W. Evans), 209–220; 1993, London, The Institute of Metals.
35. S. A. Kraft and H. Mughrabi: in 'Thermomechanical fatigue behavior of materials: second volume, ASTM STP 1263', (ed. M. J. Verrilli and M. G. Castelli), 27–40; 1996, Philadelphia, PA, American Society for Testing and Materials.
36. D. A. Boismier and H. Sehitoglu: *Trans. ASME*, 1990, **112**, 68–79.
37. O. Paris, M. Fährmann, E. Fährmann, T. M. Pollock and P. Fratzl: *Acta Mater.*, 1997, **45**, 1085–1097.
38. D. D. Pearson, F. D. Lemkey and B. H. Kear: Proc. 4th Int. Symp. on 'Superalloys', (ed. J. K. Tien *et al.*), 513–520; 1980, Metals Park, OH, American Society for Metals.
39. J. Hammer: Dr. Ing. Thesis, Kriech- und Zeitstandverhalten der einkristallinen Nickelbasis–Superlegierung SRR 99 unter besonderer Berücksichtigung der mikrostrukturellen Vorgänge und der Materialfehler, 1990, Universität Erlangen-Nürnberg.
40. H. Mughrabi, H. Feng and H. Biermann: Proc. IUTAM-Symp. on 'Micromechanics of plasticity and damage of multiphase materials', (ed. A. Pineau and A. Zaoui), 115–122; 1996, Dordrecht, Kluwer Academic Publishers.
41. S. Tian, H. Zhou, J. Zhang, H. Yang, Y. Xu and Z. Hu: *Mater. Sci. Eng. A*, 2000, **A279**, 160–165.
42. C. Carry and J.-L. Strudel: *Acta Metall.*, 1977, **25**, 767–777 and 1978, **26**, 859–870.
43. J. X. Zhang, T. Murakumo, Y. Koizumi and H. Harada: *J. Mater. Sci.*, 2003, **38**, 4883–4888.
44. Y. Koizumi, T. Kobayashi, T. Yokokawa, J. Zhang, M. Osawa, H. Harada, Y. Aoki and M. Arai: Proc. 10th Int. Symp. on 'Superalloys', (ed. K. A. Green *et al.*), 35–43; 2004, Warrendale, PA, The Minerals, Metals and Materials Society.

45. L. J. Carroll, Q. Feng and T. M. Pollock: *Met. Mater. Trans. A*, 2008, **39A**, 1291–1307.
46. H. Biermann: Habil. thesis, Ursachen und Auswirkungen der gerichteten Vergröberung (“Floßbildung”) in einkristallinen Nickelbasis–Superlegierungen, 1999, Universität Erlangen-Nürnberg.
47. R. Srinivasan, G. F. Eggeler and M. J. Mills: *Acta Mater.*, 2000, **48**, 4867–4878.
48. A. C. Yeh, C. M. F. Rae and S. Tin: Proc. 10th Int. Symp. on ‘Superalloys’, (ed. K. A. Green *et al.*); 677–685, 2004, Warrendale, PA, The Minerals, Metals and Materials Society.
49. L. J. Rowland, Q. Feng and T. M. Pollock: Proc. 10th Int. Symp. on ‘Superalloys’, (ed. K. A. Green *et al.*), 697–706; 2004, Warrendale, PA, The Minerals, Metals and Materials Society.
50. J. Svoboda and P. Lukáš: *Acta Mater.*, 1997, **45**, 125–135.
51. J. Svoboda and P. Lukáš: *Acta Mater.*, 1997, **46**, 3421–3431.
52. M. V. Nathal, R. A. MacKay and R. V. Miner: *Metall. Trans. A*, 1989, **20A**, 133–141.
53. H. Biermann, M. Strehler and H. Mughrabi: *Metall. Trans. A*, 1996, **27A**, 1003–114.
54. U. Tetzlaff and H. Mughrabi: Proc. 9th Int. Symp. on ‘Superalloys’, (eds. T. M. Pollock *et al.*), 273–282; 2000, Warrendale, PA, The Minerals, Metals and Materials Society.
55. M. Ott and H. Mughrabi: *Mater. Sci. Eng. A*, 1999, **A272**, 24–30.
56. F. C. Neuner, U. Tetzlaff and H. Mughrabi: in ‘Thermomechanical fatigue behavior of materials: (ed. M. McGaw *et al.*), Vol. 4, 112–126; 2002, Philadelphia, PA, American Society for Testing and Materials.
57. T. Murakumo, Y. Koizumi, K. Kobayashi and H. Harada: Proc. 10th Int. Symp. on ‘Superalloys’, (ed. K. A. Green *et al.*), 155–162; 2004, Warrendale, PA, The Minerals, Metals and Materials Society.
58. F. Pyczak, B. Devrient, F. C. Neuner and H. Mughrabi: *Acta Mater.*, 2005, **53**, 3879–3891.
59. F. Pyczak, B. Devrient and H. Mughrabi: Proc. 10th Int. Symp. on ‘Superalloys’, (eds. K. A. Green *et al.*), 827–836; 2004, Warrendale, The Minerals, Metals and Materials Society.
60. C. L. Fu, R. Reed, A. Janooti and M. Kremar: Proc. 10th Int. Symp. on ‘Superalloys’, (ed. K. A. Green *et al.*), 867–876; 2004, Warrendale, PA, The Minerals, Metals and Materials Society.
61. S. Walston, A. Cetel, R. Mra, D. Duhl and R. Dreshfield: Proc. 10th Int. Symp. on ‘Superalloys’, (ed. K. A. Green *et al.*), 15–24; 2004, Warrendale, PA, The Minerals, Metals and Materials Society.
62. Y. Koizumi, T. Kobayashi, T. Yokokawa, J. Zhang, M. Osawa, H. Harada, Y. Aoki and M. Arai: Proc. 10th Int. Symp. on ‘Superalloys’, (ed. K. A. Green *et al.*), 35–43; 2004, Warrendale, PA, The Minerals, Metals and Materials Society.
63. A. Dlouhy, M. Probst-Hein and G. Eggeler: *Mater. Sci. Eng. A*, 2001, **A309–310**, 278–282.
64. A. Epishin and T. Link: *Philos. Mag.*, 2004, **84**, 1979–2000.